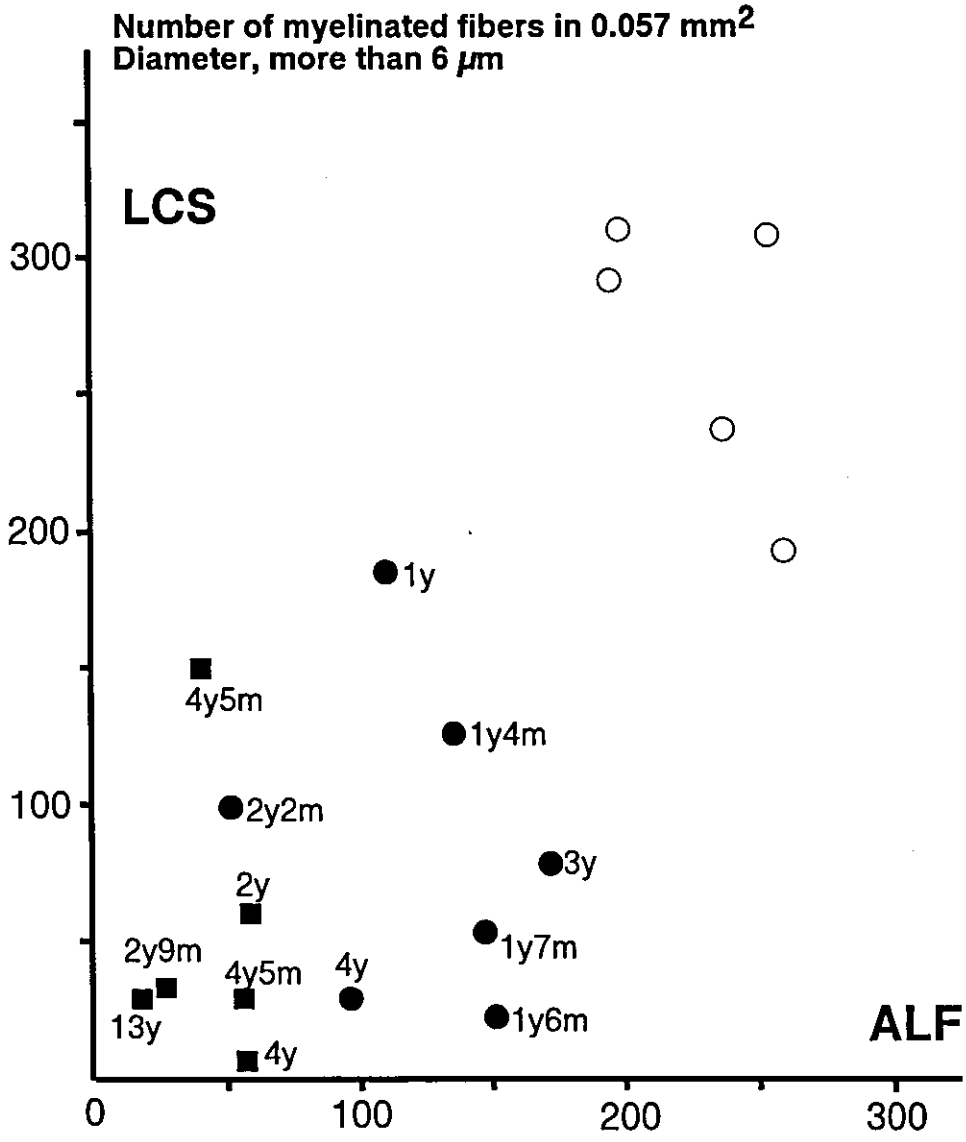


Fig. 10. Oyanagi et al.

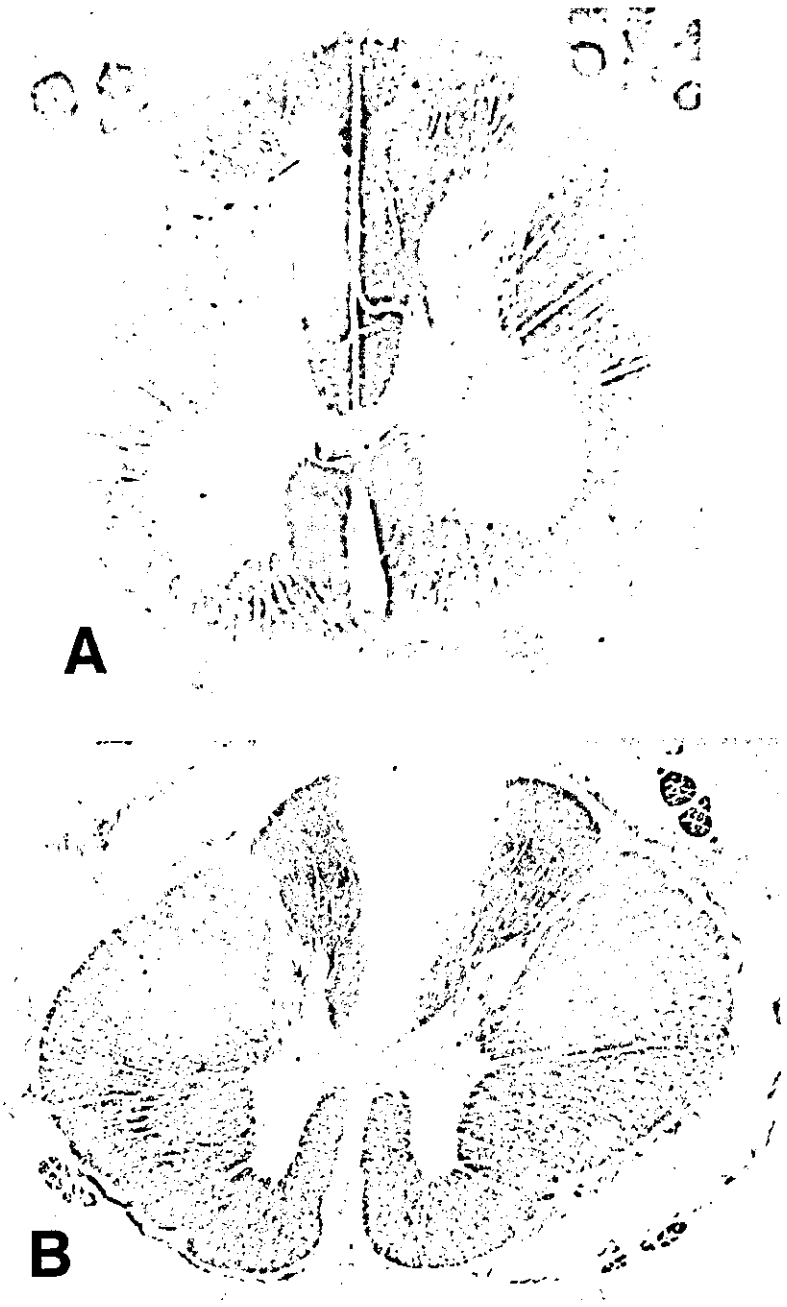


Fig. 11. Oyanagi et al.

Journal of Neuroscience Research 75:678–687 (2004)

# Distinctive Expression of Midkine in the Repair Period of Rat Brain During Neurogenesis: Immunohistochemical and Immunoelectron Microscopic Observations

**Kae Kikuchi-Horie,[1,2] Emiko Kawakami,[1] Makiko Kamata,[3] Manabu Wada,[1,4] Jian-Guo Hu,[3] Hachiro Nakagawa,[3] Kazuhiko Ohara,[1,2] Kazuhiko Watabe,[5] and Kiyomitsu Oyanagi[1]***

[1]Department of Neuropathology, Tokyo Metropolitan Institute for Neuroscience, Tokyo, Japan
[2]Department of Veterinary Anatomy, Faculty of Agriculture, Tokyo University of Agriculture and Technology, Tokyo, Japan
[3]Research and Development Center, BML, Saitama, Japan
[4]The Third Department of Internal Medicine, Yamagata University School of Medicine, Yamagata, Japan
[5]Molecular Neuropathology, Tokyo Metropolitan Institute for Neuroscience, Tokyo, Japan

Distinctive expression of midkine (MK) was observed during the repair period of fetal brain neuroepithelium. MK is a heparin-binding growth factor that occurs as a product of a retinoic acid-inducible gene, and has a molecular mass of 13 kDa. MK expression was examined immunohistochemically and by immunoelectron microscopy during a period of repair in developing rat brain at the neurogenesis stage. Injury was induced in rat fetuses by transplacental administration of ethylnitrosourea (ENU) on embryonic Day (E) 16, and histological changes were examined up to 48 hr thereafter (i.e., up to E 18). In normal rat fetuses, MK immunostaining was observed in the cytoplasm and radial and horizontal processes of all cells in the neuroepithelium (NE), subventricular zone (SV), and intermediate zone (IMZ). In ENU-administered brains, cells in the NE, SV, and IMZ were damaged severely, especially 16–24 hr after ENU administration. The remaining neuroepithelial cells, with the exception of those in M-phase and the tips of processes at the ventricular surface, were negative for MK immunohistochemistry 16–24 hr after the administration of ENU. Forty-eight hours after the administration, the cytoplasm and processes of cells in the NE, SV, and IMZ were MK immunopositive. Our previous data reported that the cell cycle of most NE cells is synchronized to the S-phase 16 hr after ENU administration and to the M-phase at 24 hr, and many NE cells were recovered 48 hr after ENU administration. The previous results taken together with the present results indicate that: (1) MK expression does not increase during the repair period of the NE, being different from adults; (2) MK expression is likely to be suppressed at S-phase according to the condition of the NE; and (3) MK expression is not essential for every cell cycle phase of NE cells; but (4) is necessary to maintain the M-phase of NE cells. 

**Key words:** cell cycle; ethylnitrosourea; lesion repair; midkine; neuroepithelium

Midkine (MK) is a heparin-binding growth factor that occurs as a product of a retinoic acid-inducible gene, and has a molecular mass of 13 kDa (Muramatsu, 1994). MK has been reported as involved in neurogenesis and neuron differentiation, in neurite outgrowth (Michikawa et al., 1993; Muramatsu et al., 1993; Matsuzawa et al., 1999), and neuronal survival (Michikawa et al., 1993; Satoh et al., 1993; Matsuzawa et al., 1999). In the developing brain, MK has been reported to occur in the neuroepithelium (NE) (Muramatsu et al., 1993; Mitsiadis et al., 1995), migrating neurons, and processes of radial glia (Matsumoto et al., 1994; Sun et al., 1997, 1999). The MK receptor-like protein tyrosine phosphatase PTPζ/RPTPβ has been observed in migrating neurons and processes of radial glia of the fetal rat brain, suggesting the involvement of MK in neuroblast migration (Maeda and Noda, 1998; Maeda et al., 1999). MK has also been detected in various organs during the mid-gestation period of embryogenesis and is considered to be involved in regulation of organogenesis (Kadomatsu et al., 1990; Mitsiadis et al., 1995). MK expression decreases gradually with age, and in normal adult mice is expressed persistently only in the kidney

Jian-Guo Hu is currently at Fuji Photo Optical Co., Saitama, Japan.

*Correspondence to: Kiyomitsu Oyanagi, MD, PhD, Department of Neuropathology, Tokyo Metropolitan Institute for Neuroscience, 2-6 Musashidai, Fuchu, Tokyo 183-8526, Japan. E-mail: k123ysm@tmin.ac.jp

Received 28 July 2003; Revised 6 November 2003; Accepted 19 November 2003

**Published online 2 February 2004 in Wiley InterScience (www.interscience.wiley.com). DOI: 10.1002/jnr.20015**

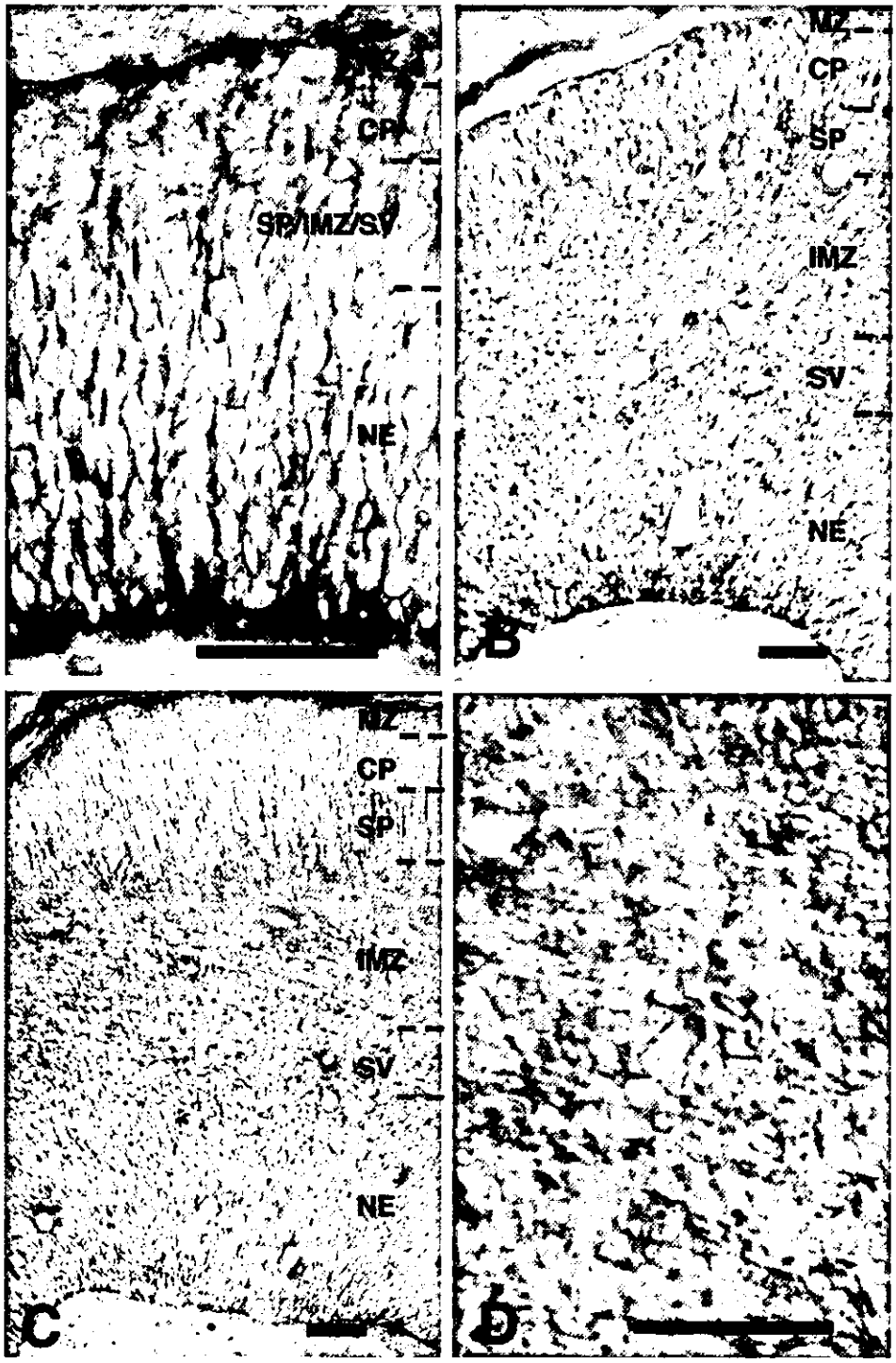


Fig. 3. Immunohistochemistry for MK in the dorsal cerebral neocortex of control animals E 16–18. Counterstained with methyl green. (**A**) Normal E 16; (**B**) normal E 17; (**C**) normal E 18; (**D**) intermediate zone (IMZ) of normal E 18. NE, neuroepithelium; SV, subventricular zone; IMZ, intermediate zone; SP, subplate; CP, cortical plate; MZ, marginal zone. Scale bars = 50 μm.

brain tissue of normal and ENU-administered rats (Fig. 2B). Although the data obtained were not significant statistically, the amount of MK in the normal fetal brain showed a tendency to decrease with development from E 16 to E 18 (Fig. 2C). An increase in MK was not evident in brains of ENU-treated rat fetuses (Fig. 2D).

## MK Immunohistochemistry

Strong MK immunoreactivity in the normal fetal brain was observed in cytoplasm and processes of all cells in the NE, SV, and IMZ on E 15 and 16 (Fig. 3A). MK immunoreactivity was relatively strong in cell processes, perpendicular and horizontal to the ventricle wall, in the

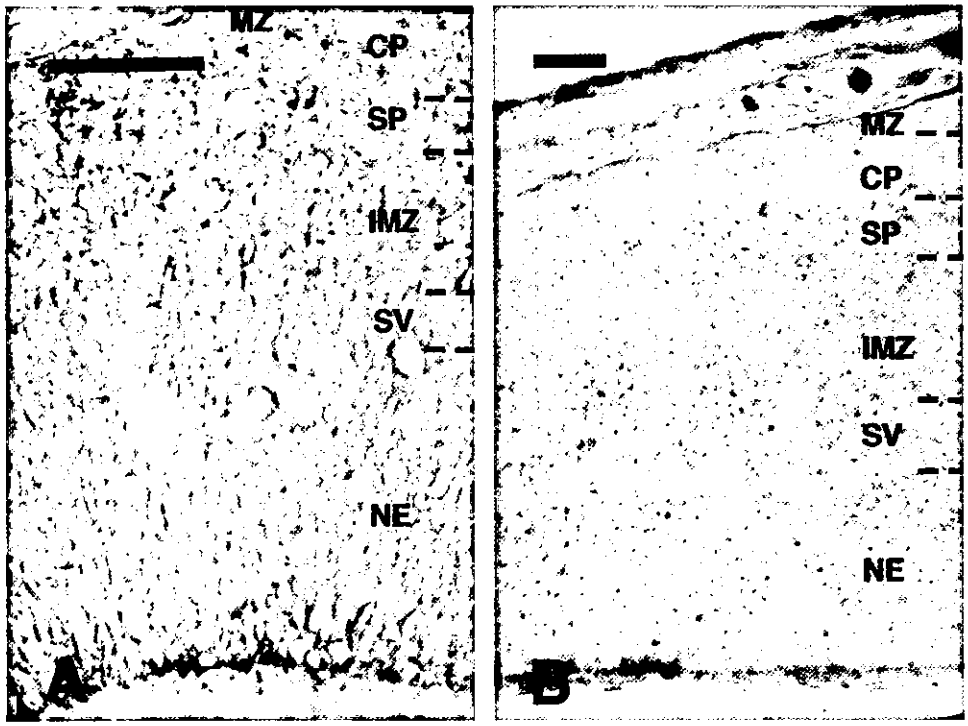


Fig. 4. Immunohistochemistry for MK in the dorsal cerebral neocortex 8 (A) and 16 hr (B) after ENU injection. Counterstained with methyl green. In ENU-treated rat fetuses 8 hr after administration, MK-immunoreactivity in cytoplasm and processes of the cells in the NE, SV, and IMZ was weaker than that of normal E 16 tissue. Sixteen hours after ENU administration, immunoreactivity in cytoplasm and processes in the NE, SV, and IMZ was weak, but fine granular immunoreactivity appeared in the IMZ and NE. NE, neuroepithelium; SV, subventricular zone; IMZ, intermediate zone; SP, subplate; CP, cortical plate; MZ, marginal zone. Scale bars = 50 μm.

IMZ on E 17 and 18 (Fig. 3B–D). MK immunopositivity was not seen in the nuclei (Fig. 3A–D) or the cytoplasm of cells in the CP (Fig. 3B,C).

In the ENU-treated rat fetuses 8 hr after administration, MK immunoreactivity in the cytoplasm and processes of the cells in the NE, SV, and IMZ was weaker than that of normal E 16 tissue (Fig. 4A). Sixteen hours after ENU administration, immunoreactivity in cytoplasm and processes in the NE, SV, and IMZ was weak, but fine granular immunoreactivity appeared in the IMZ and NE (Fig. 4B). Twenty-four hours after ENU administration, the amount of fine granular MK immunoreactivity had increased further, and MK-immunopositive cytoplasm and processes of the cells in the NE, SV, and IMZ were observed only rarely (Fig. 5A). MK immunoreactivity was abolished completely by omitting the anti-MK antibody (Fig. 5B). Immunoelectron microscopic observation of MK revealed strong immunoreactivity in the cytoplasm and cell processes of NE cells and migrating neuroblasts in the IMZ of normal E 17 fetal brain. All cell processes in the NE and IMZ were positive for MK immunostaining (data not shown). Conversely, no immunostaining was seen in the cytoplasm and processes of migrating neuroblasts, NE cells, and radial glia 24 hr after ENU administration. Only the cytoplasm of NE cells in the M-phase and processes along the ventricular surface were densely immunopositive for MK 24 hr after ENU administration (Fig. 5C). Fine granular MK immunostaining was localized exclusively within apoptotic cells, but not observed in normal-looking cells in the NE, SV, and IMZ (Fig. 5D).

The amount of fine granular immunoreactivity of MK had decreased 36 hr after ENU administration, and MK immunoreactivity in the IMZ, corresponding to migrating neuroblasts and NE cells and processes were stronger than that observed at 16 and 24 hr. Clustering of MK-immunopositive material in the IMZ (Fig. 6A,B) considered to be phagocytes containing apoptotic cells observed previously (Oyanagi et al., 1986). Fine granular immunoreactivity was greatly decreased 48 hr after ENU administration, and cytoplasm and processes of all cells in the NE, SV, and IMZ were immunopositive for MK (Fig. 6B). NE cells along with ventricular surface, which are considered to be in M-phase, were positive for MK-immunohistochemistry at each period during the observation (Fig. 3–6). Neither the nuclei nor the cytoplasm of cortical plate cells were immunopositive for MK (Fig. 3–5).

## DISCUSSION

ENU is known to be a neurogenic resorptive carcinogen (Druckrey et al., 1972; Bosch, 1977a), and to have a cytotoxic effect immediately after administration (Bosch et al., 1972). ENU has been reported to impair cellular DNA synthesis by alkylating the bases, and to decompose in intact animals with a half-life of less than 20 min (Swann and Magee, 1971). ENU has been found to induce selective degeneration of proliferating cells (Bosch, 1977b) or cells in the S- to M-phase of the cell cycle in developing brain (Yoshida et al., 1984), and temporary cell-cycle arrest in or before the S-phase (Bosch and Ebels, 1976). Transplacental ENU administration to fetuses has been reported to result in microcephalus, paucity of dendrites, and a reduction in neuronal cytoplasm in the central nervous system (Hallas and Das, 1978, 1979),

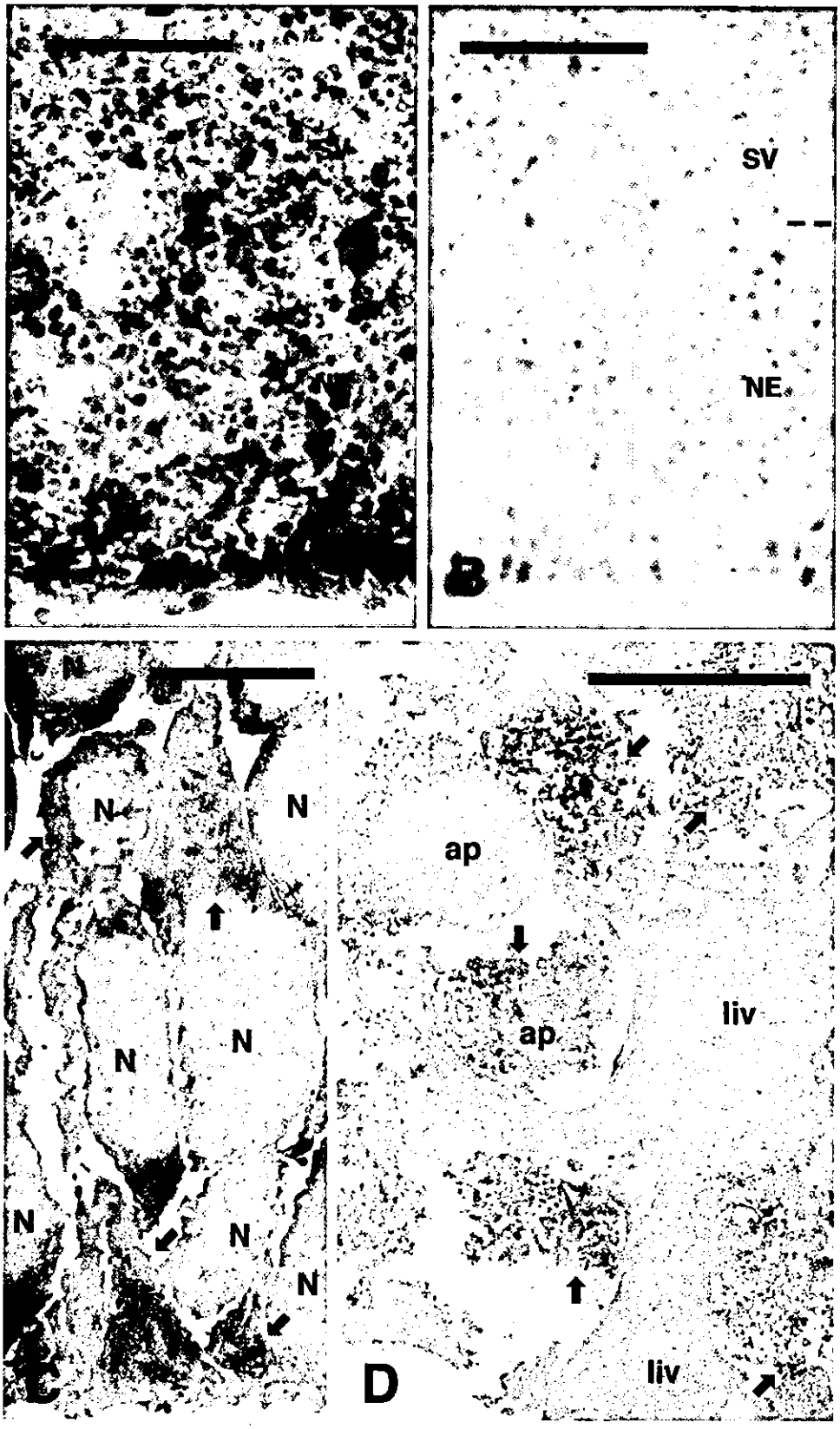


Fig. 5. Immunohistochemistry for MK in the neuroepithelium (NE) and subventricular zone (SV) at the dorsal cerebral neocortex 24 hr after ENU injection. **A:** NE; amount of fine granular MK immunoreactivity had increased further and MK-immunopositive cytoplasm and cell processes in the NE, SV, and IMZ were observed only rarely. **B:** MK immunoreactivity is abolished completely by omitting anti-MK antibody. Scale bars = 50 μm. Immunoelectron microscopic findings of MK-immunohistochemistry. **C:** Ventricular surface of NE 24 hr after ENU administration. **D:** NE 24 hr, only the cytoplasm of NE cells in the M-phase and processes along ventricular surface were densely immunopositive for MK. Fine granular MK-immunostaining was localized exclusively within the apoptotic cells, but not observed in normal looking cells in the NE, SV, and IMZ. Arrowheads, MK immunoreactivity; N, nucleus; liv, normal-looking cell; ap, apoptotic cell. Scale bars = 5 μm.

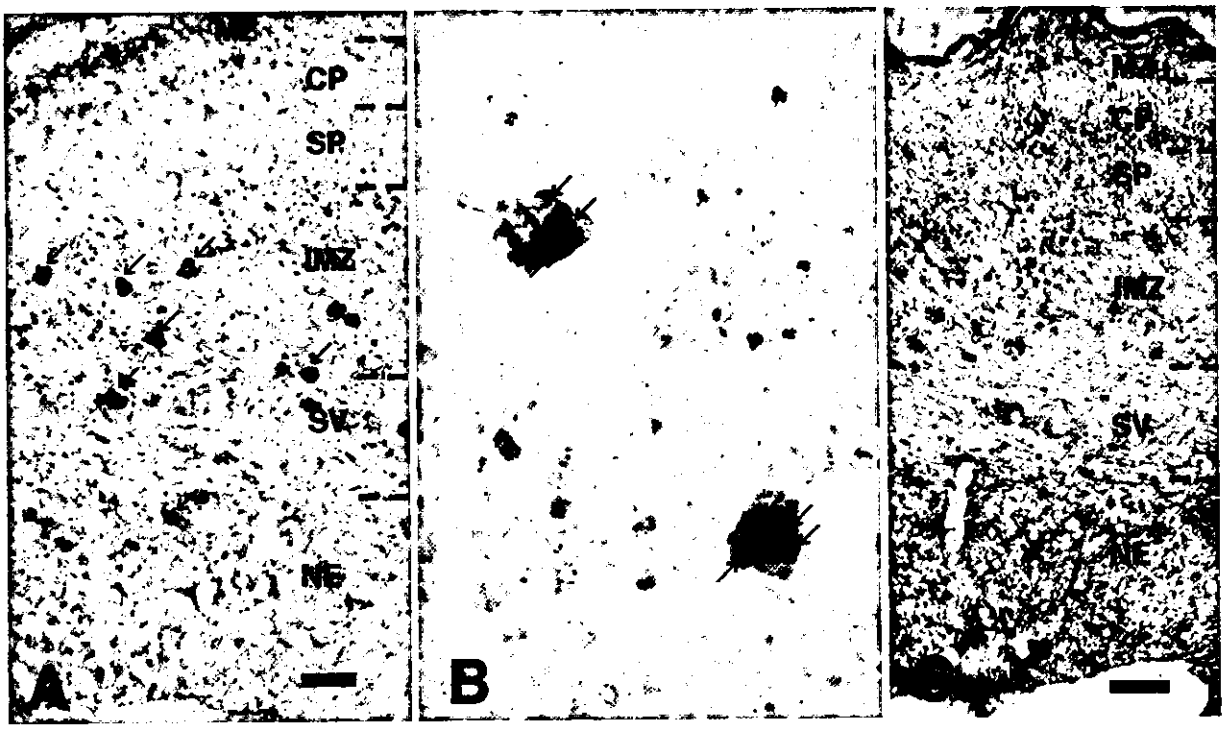


Fig. 6. Immunohistochemistry for MK in dorsal cerebral neocortex 36 and 48 hr after ENU injection. **A:** Arrows indicate clustering of MK-immunopositive material. **B:** High-power view of A. Arrows show nuclei of MK-immunopositive cells. Counterstained with methyl green. A and B, 36 hr; C, 48 hr. NE, neuroepithelium; SV, subventricular zone; IMZ, intermediate zone; SP, subplate; CP, cortical plate; MZ, marginal zone. Scale bars = 50 μm.

and the severity of fatal brain tissue damage is controllable by the amount of ENU (Fujiwara, 1980; Yoshida et al., 1984).

During neurogenesis, the NE of spinal cord and the external granular cell layer of cerebellum are able to regenerate within a certain period after injury (Altman et al., 1969; Shimada and Langman, 1970; Houle and Das, 1984; Ferrer et al., 1995). It has been reported previously that ENU administration (60 mg/kg body weight) to the developing rat brain at the neurogenesis stage results in: (1) severe damage to NE cells, migrating neuroblasts, and processes of radial glia, especially 16–24 hr after administration; (2) temporary arrest of NE cell cycle in the G1-phase 4–8 hr after administration; (3) cell cycle synchronization of most NE cells to the S-phase at 16 hr after administration and to the M-phase 24 hr thereafter; and (4) recovery of many cells in the NE 48 hr after administration of ENU (Oyanagi et al., 1998).

In the present study, MK was expressed continuously in the cytoplasm of the NE cells, radial and perpendicular processes, and in the postmitotic migrating neuroblasts, but disappeared in the cytoplasm of immature neurons after arriving at the cortical plate in the normal developing brain. During the repair period of the developing brain, however, fine granular MK immunostaining was localized exclusively within apoptotic cells but not observed in normal-looking cells in the NE, SV, and IMZ 24 hr after ENU administration. This indicates that MK expression was suppressed in the living NE cells, when most NE cells are in the S- to G2-phase (Oyanagi et al., 1998). NE cells in the M-phase and the tips of cell processes at the ventricular surface, however, were always positive for MK immunohistochemistry. This shows that MK is necessary for the M-phase of NE cells and that MK might be essential for keeping junctional complex of NE cells (Fig. 7). Continuous MK expression in NE cells at the M-phase may relate to the potential function of MK to induce cell proliferation (Ratovitski et al., 1998; Kato et al., 1999; Qiu et al., 2000).

In the normal fetal brain at the neurogenesis stage, all processes of cells in NE and IMZ were immunopositive for MK; thus, "radial glia", if they would exist, are positive for MK immunohistochemistry. It was observed in the present study that after ENU administration, alteration of MK expression in cells and processes in the NE was quite synchronized. This finding suggests that ENU promotes synchronization of the kinetics of NE cells and radial glia, if any, or that the processes of radial glia are the processes of the NE cells (Fujita, 1963; Fujita and Fushiki, 1983; Ikuta et al., 1984) (Fig. 7).

MK has been reported to be a secreted protein (Muramatsu and Muramatsu, 1991). In the present study and as reported previously, however, MK immunostaining was observed exclusively inside cells. This finding may be

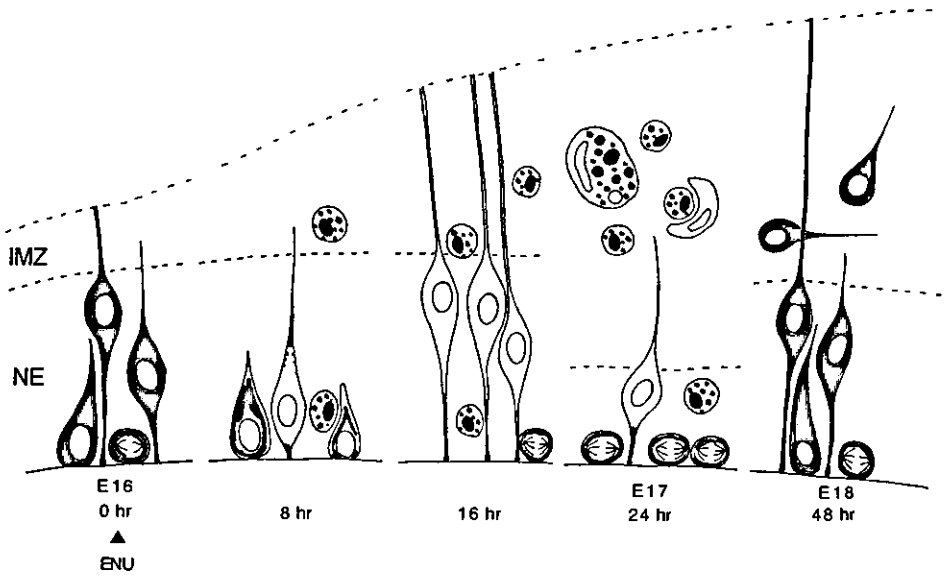


Fig. 7. Schematic demonstration of MK expression (orange) in early stage of repair process of developing rat brain at neurogenesis. Bipolar or unipolar cells are NE cells or migrating neuroblasts; round cells showing mitosis along ventricular wall are NE cells in M-phase, and round cells containing MK-immunopositive granules are apoptotic cells. IMZ, intermediate zone; NE, neuroepithelium.

the result of internalization of secreted MK into the cytoplasm (Ohta et al., 1999), and washing out of the MK from the extracellular spaces during rinsing of sections in the immunohistochemistry protocol.

The findings of the neuroepithelial cells observed in the present study indicate that: (1) MK expression does not increase during the repair period of the neuroepithelium, being different from adults; (2) MK expression is likely to suppressed at the S-phase according to the condition of the neuroepithelium; and (3) MK expression is not essential for every phase of the cell cycle of neuroepithelial cells; but (4) is necessary to maintain the M-phase of the neuroepithelial cells (Fig. 7).

## ACKNOWLEDGMENTS

We thank Ms. Y. Kawazoe of the Department of Molecular Neuropathology and Ms. A. Nakamura of the Department of Neuropathology (Tokyo Metropolitan Institute for Neuroscience) for technical advice. We also thank Dr. H. Kawano and Dr. M. Horie of the Department of Anatomy and Development (Tokyo Metropolitan Institute for Neuroscience) for their help, and Dr. H. Shibata and Professor N. Kanda of the Faculty of Agriculture, Tokyo University of Agriculture and Technology for allowing us the opportunity to carry out this research.

## REFERENCES

Altman J, Anderson WJ, Write KA. 1969. Reconstitution of the external granular cell layer of the cerebellar cortex in infant rats after low-level X-irradiation. Anat Rec 163:453–472.

Bayer SA, Altman J. 1991. Neocortical development. New York: Raven Press.

Bosch DA. 1977a. Short and long term effects of methyl- and ethylnitrosourea (MNU and ENU) on the developing nervous system of the rat. I. Long term effects: the induction of (multiple) gliomas. Acta Neurol Scand 55:85–105.

Bosch DA. 1977b. Short and long term effects of methyl- and ethylnitrosourea (MNU and ENU) on the developing nervous system of the rat. II. Short term effects: concluding remarks on chemical neuro-oncogenesis. Acta Neurol Scand 55:106–122.

Bosch DA, Ebels EJ. 1976. Temporary cell cycle arrest in neural and extraneural developing rat tissues after exposure to methyl and ethylnitrosourea. Z Krebsforsch Klin Onkol Cancer Res Clin Oncol 86:23–31.

Bosch DA, Gerrits PO, Ebels EJ. 1972. The cytotoxic effect of ethylnitrosourea and methylnitrosourea on the nervous system of the rat at different stages of development. Z Krebsforsch Klin Onkol Cancer Res Clin Oncol 77:308–318.

Boulder Committee. 1970. Embryonic vertebrate central nervous system: revised terminology. Anat Rec 166:257–262.

Druckrey H, Ivankovic S, Preussmann R, Zülch KJ, Mennel HD. 1972. Selective induction of malignant tumors of the nervous system by resorptive carcinogen. In: Kirsch WM, Grossi-Paoletti E, Paoletti P, editors. The experimental biology of brain tumors. Springfield, IL: Charles C Thomas. p 85–147.

Ferrer I, Barrón S, Rodríquez-Farré E, Planas AM. 1995. Ionizing radiation-induced apoptosis is associated with c-Jun expression and c-Jun/AP-1 activation in the developing cerebellum of the rat. Neurosci Lett 202:105–108.

Fujita S. 1963. The matrix cell and cytogenesis in the developing central nervous system. J Comp Neurol 120:37–42.

Fujita S, Fushiki S. 1983. [Significance of cell movement in the histogenesis of the nervous system]. Tanpakushitsu Kakusan Koso 28:469–487.

Fujiwara H. 1980. Cytotoxic effects of ethylnitrosourea on central nervous system of rat embryos. Special references to carcinogenesis and teratogenesis. Acta Pathol Jpn 30:375–387.

Hallas BH, Das GD. 1978. *N*-ethyl-*N*-nitrosourea-induced teratogenesis of brain in the rat. J Neurol Sci 39:111–122.

Hallas BH, Das GD. 1979. An aberrant nucleus in the telencephalon following administration of ENU during neuroembryogenesis. Teratology 19:159–164.

Houle JD, Das GD. 1984. Tissue repair in the embryonic rat spinal cord following exposure to *N*-ethyl-*N*-nitrosourea. Int J Dev Neurosci 2:1–11.

Ikuta F, Yoshida Y, Ohama E, Oyanagi K, Takeda S, Yamazaki K, Watabe K. 1984. Brain and peripheral nerve edema as an initial stage of the lesion repair: revival of the mechanisms of the normal development in the fetal brain. Shinkei Kenkyu No Shimpo 28:599–628.

Kadomatsu K, Huang RP, Suganuma T, Murata F, Muramatsu T. 1990. A retinoic acid responsive gene MK found in the teratocarcinoma system is expressed in spatially and temporally controlled manner during mouse embryogenesis. J Cell Biol 110:607–616.

Kato S, Ishihara K, Shinozawa T, Yamaguchi H, Asano Y, Saito M, Kato M, Terada T, Awaya A, Hirano A, Dickson DW, Yen SH, Ohama E. 1999. Monoclonal antibody to human midkine reveals increased midkine expression in human brain tumors. J Neuropathol Exp Neurol 58:430–441.

Maeda N, Ichihara-Tanaka K, Kimura T, Kadomatsu K, Muramatsu T, Noda M. 1999. A receptor-like protein-tyrosine phosphatase PTPζ/RPTPβ binds a heparin-binding growth factor midkine. J Biol Chem 274:12474–12479.

Maeda N, Noda M. 1998. Involvement of receptor-like protein tyrosine phosphataseζ/RPTPβand its ligand pleiotrophin/heparin-binding growth-associated molecule (HB-GAM) in neuronal migration. J Cell Biol 142:203–216.

Maekawa T, Waki S, Okada A, Fukui H, Kinoshita Y, Chiba T. 1999. Midkine gene expression in the healing process of gastric ulcer. J Lab Clin Med 133:349–352.

Matsumoto K, Wanaka A, Takatsuji K, Muramatsu H, Muramatsu T, Tohyama M. 1994. A novel family of heparin-binding growth factors, pleiotrophin and midkine, is expressed in the developing rat cerebral cortex. Brain Res Dev Brain Res 79:229–241.

Matsuzawa M, Muramatsu T, Yamamori T, Knoll W, Yano R. 1999. Novel neuronal effects of midkine on embryonic cerebellar neurons examined using a defined culture system. Cell Mol Neurobiol 19:209–221.

Michikawa M, Kikuchi S, Muramatsu H, Muramatsu T, Kim SU. 1993. Retinoic acid responsive gene product, midkine, has neurotrophic functions for mouse spinal cord and dorsal root ganglion neurons in culture. J Neurosci Res 35:530–539.

Mitsiadis TA, Salmivirta M, Muramatsu T, Muramatsu H, Rauvala H, Lehtonen E, Jalkanen M, Thesleff I. 1995. Expression of the heparin-binding cytokines, midkine (MK) and HB-GAM (pleiotrophin) is associated with epithelial-mesenchymal interactions during fetal development and organogenesis. Development 121:37–51.

Mochizuki R, Takeda A, Sato N, Kimpara T, Onodera H, Itoyama Y, Muramatsu T. 1998. Induction of midkine expression in reactive astrocytes following rat transient forebrain ischemia. Exp Neurol 149:73–78.

Muramatsu T. 1994. The midkine family of growth/differentiation factors. Dev Growth Differ 36:1–8.

Muramatsu H, Muramatsu T. 1991. Purification of recombinant midkine and examination of its biological activities: functional comparison of new heparin binding factors. Biochem Biophys Res Commun 177:652–658.

Muramatsu H, Shirahama H, Yonezawa S, Maruta H, Muramatsu T. 1993. Midkine, a retinoic acid-inducible growth/differentiation factor: immunochemical evidence for the function and distribution. Dev Biol 159:392–402.

Nakamoto M, Matsubara S, Miyauchi T, Obama H, Ozawa M, Muramatsu T. 1992. A new family of heparin binding growth/differentiation factors: differential expression of the midkine (MK) and HB-GAM genes during mouse development. J Biochem 112:346–349.

Ohta S, Muramatsu H, Senda T, Zou K, Iwata H, Muramatsu T. 1999. Midkine is expressed during repair of bone fracture and promotes chondrogenesis. J Bone Miner Res 14:1132–1144.

Oyanagi K, Kakita A, Kawasaki K, Hayashi S, Yamada M. 2001. Expression of calbindin D-28k and parvalbumin in cerebral cortical dysgenesis induced by administration of ethylnitrosourea to rats at the stage of neurogenesis. Acta Neuropathol 101:375–382.

Oyanagi K, Kakita A, Yamada M, Kawasaki K, Hayashi S, Ikuta F. 1998. Process of repair in the neuroepithelium of developing rat brain during neurogenesis: chronological and quantitative observation of DNA-replicating cells. Brain Res Dev Brain Res 108:229–238.

Oyanagi K, Yoshida Y, Ikuta F. 1986. The chronology of lesion repair in the developing rat brain: biological significance of the preexisting extracellular space. Virchows Arch A Pathol Anat Histopathol 408:347–359.

Oyanagi K, Yoshida Y, Ikuta F. 1987. Selectivity of cell degeneration and histological peculiarities of the repair process in the developing rat spinal cord after ethylnitrosourea administration. Brain Nerve 39:1077–1082.

Oyanagi K, Yoshida Y, Ikuta F. 1988. Cyto-architectonic investigation of the rat spinal cord following ethylnitrosourea administration at different developmental stages. Virchows Arch A Pathol Anat Histopathol 412:215–224.

Qiu L, Escalante CR, Aggarwal AK, Wilson PD, Burrow CR. 2000. Monomeric midkine induces tumor cell proliferation in the absence of cell-surface proteoglycan binding. Biochemistry 39:5977–5987.

Paxinos G, Ashwell KWS, Törk I. 1994. Atlas of the developing rat nervous system, Second ed. San Diego: Academic Press.

Ratovitski EA, Kotzbauer PT, Milbrandt J, Lowenstein CJ, Burrow CR. 1998. Midkine induces tumor cell proliferation and binds to a high affinity signaling receptor associated with JAK tyrosine kinases. J Biol Chem 273:3654–3660.

Satoh J, Muramatsu H, Moretto G, Muramatsu T, Chang HJ, Kim ST, Cho JM, Kim SU. 1993. Midkine that promotes survival of fetal human neurons is produced by fetal human astrocytes in culture. Brain Res Dev Brain Res 75:201–205.

Shimada M, Langman J. 1970. Repair of the external granular layer of the hamster cerebellum after prenatal and postnatal administration of methylazoxymethanol. Teratology 3:119–134.

Sun XZ, Inouye M, Fukui Y, Hisano S, Sawada K, Muramatsu H, Muramatsu T. 1997. An immunohistochemical study of radial glial cells in the mouse brain prenatally exposed to γ-irradiation. J Neuropathol Exp Neurol 56:1339–1348.

Sun XZ, Takahashi S, Fukui Y, Hisano S, Kuboda Y, Sato H, Inouye M. 1999. Different patterns of abnormal neuronal migration in the cerebral cortex of mice prenatally exposed to irradiation. Brain Res Dev Brain Res 114:99–108.

Swann PF, Magee PN. 1971. Nitrosamine-induced carcinogenesis. The alkylation of N-7 of guanine of nucleic acids of the rat by diethylnitrosamine, *N*-ethyl-*N*-nitrosourea and ethyl methanesulphonate. Biochem J 125:841–847.

Wada M, Kamata M, Aizu Y, Morita T, Hu JG, Oyanagi K. 2002. Alteration of midkine expression in the ischemic brain of humans. J Neurol Sci 200:67–73.

Wang SY, Yoshida Y, Goto M, Moritoyo T, Tsutsui J, Izumo S, Sato E, Muramatsu T, Osame M. 1998. Midkine exists in astrocytes in the early stage of cerebral infarction. Brain Res Dev Brain Res 106:205–209.

Yoshida Y, Goto M, Tsutsui J, Ozawa M, Sato E, Osame M, Muramatsu T. 1995. Midkine is present in the early stage of cerebral infarct. Brain Res Dev Brain Res 85:25–30.

Yoshida Y, Oyanagi K, Ikuta F. 1984. Initial cellular damage in the developing rat brain caused by cytotoxicity of ethylnitrosourea. Brain Nerve 36:175–182.

Acta Neuropathologica

DOI 10.1007/s00401-004-0971-7

Regular Paper

# *Klotho* insufficiency causes decrease of ribosomal RNA gene transcription activity, cytoplasmic RNA and rough ER in the spinal anterior horn cells

**Yorito Anamizu · Hiroshi Kawaguchi · Atsushi Seichi · Shinji Yamaguchi · Emiko Kawakami · Naotoshi Kanda · Shiro Matsubara · Makoto Kuro-o · Yoichi Nabeshima · Kozo Nakamura · Kiyomitsu Oyanagi (✉)**

Y. Anamizu · E. Kawakami · K. Oyanagi
Department of Neuropathology, Tokyo Metropolitan Institute for Neuroscience, 2-6 Musashidai, Fuchu, 183-8526 Tokyo, Japan

Y. Anamizu · H. Kawaguchi · A. Seichi · K. Nakamura
Department of Orthopedic Surgery, Graduate School of Medicine, University of Tokyo, Tokyo, Japan

S. Yamaguchi
Department of Biochemistry, Molecular Biology and Cell Biology, Northwestern University, Evanston, Illinois, USA

N. Kanda
Department of Anatomy, School of Veterinary Medicine, Tokyo University of Agriculture and Technology, Tokyo, Japan

S. Matsubara
Department of Neurology, Tokyo Metropolitan Neurological Hospital, Fuchu, Tokyo, Japan

M. Kuro-o
Department of Pathology, University of Texas Southwestern Medical Center, Dallas, Texas, USA

Y. Nabeshima
Department of Tumor Biology, Graduate School of Medicine, Kyoto University, Kyoto, Japan

✉ K. Oyanagi
Phone: +81-42-3253881 ext 4711
Fax: +81-42-3218678
E-mail: k123ysm@tmin.ac.jp

**Received:** 8 September 2004 / **Revised:** 29 November 2004 / **Accepted:** 29 November 2004

Journal: *Acta Neuropathologica*
DOI: 10.1007/s00401-004-0971-7

# Offprint Order Form

- To determine if your journal provides free offprints, please check the journal's instructions to authors.
- You are entitled to a PDF file **if you order offprints.**
- Please specify where to send the PDF file:

❑ k123ysm@tmin.ac.jp

❑ _____

- If you do not return this order form, we assume that you do not wish to order offprints.
- If you order offprints **after** the issue has gone to press, costs are much higher. Therefore, we can supply offprints only in quantities of 300 or more after this time.
- For orders involving more than 500 copies, please ask the production editor for a quotation.

## Please note that orders will be processed only if a credit card number has been provided. For German authors, payment by direct debit is also possible.

**Please enter my order for:**

| | Copies | Price EUR | Price USD |
|---|---|---|---|
| ❑ | 50 | 300.00 | 330.00 |
| ❑ | 100 | 365.00 | 405.00 |
| ❑ | 200 | 525.00 | 575.00 |
| ❑ | 300 | 680.00 | 750.00 |
| ❑ | 400 | 855.00 | 940.00 |
| ❑ | 500 | 1,025.00 | 1,130.00 |

I wish to be charged in ❑ Euro ❑ USD

Prices include surface mail postage and handling. Customers in EU countries who are not registered for VAT should add VAT at the rate applicable in their country.

VAT registration number (EU countries only):

_____

**Please charge my credit card**
- ❑ **Eurocard/Access/Mastercard**
- ❑ **American Express**
- ❑ **Visa/Barclaycard/Americard**

**Number (incl. check digits):**

_ _ _ _ _ _ _ _ _ _ _ _ _ _ _ _ _ _ _

**Valid until:** _ _ / _ _

**Date / Signature:** _____

**For authors resident in Germany: payment by direct debit:**
**I authorize Springer to debit the amount owed from my bank account at the due time.**

**Account no.:** _____

**Bank code:** _____

**Bank:** _____

**Date / Signature:** _____

**Send receipt to:**

❑ Kiyomitsu Oyanagi
Tokyo Metropolitan Inst. Neuroscience
Department of Neuropathology
2-6 Musashidai
Tokyo
183-8526, Japan

❑ _____

**Ship offprints to:**

❑ Kiyomitsu Oyanagi
Tokyo Metropolitan Inst. Neuroscience
Department of Neuropathology
2-6 Musashidai
Tokyo
183-8526, Japan

❑ _____

**Abstract** The *klotho* gene was identified in 1997 as the gene whose severe insufficiency (*kl/kl*) causes a syndrome resembling human aging, such as osteoporosis, arteriosclerosis, gonadal atrophy, emphysema, and short life span in a mouse strain. Regarding the gait disturbance reported in *kl/kl* mice, the present study examined the spinal cord of *kl/kl* mice, and revealed decreases in the number of large anterior horn cells (AHCs), the amount of cytoplasmic RNA, the number of ribosomes and rough endoplasmic reticulum (rER), and the activity of ribosomal (r) RNA gene transcription without significant loss of the total number of neurons in the ventral gray matter. Increased immunostaining of phosphorylated neurofilament in the AHCs and of glial fibrillary acidic protein in reactive astrocytes in the anterior horn of *kl/kl* mice were also observed. On the other hand, the posterior horn was quite well preserved. The results suggest that the *kl/kl* insufficiency causes atrophy and dysfunction of the spinal AHCs through decreased activity of rRNA gene transcription, which may reduce the amount of cytoplasmic RNA and the number of ribosomes and rER. These findings resemble those found in the spinal cord of patients with classic amyotrophic lateral sclerosis (ALS). The results show that *klotho* gene insufficiency causes dysfunction of the protein synthesizing system in the AHCs, and might indicate the *klotho* gene is involved in the pathological mechanism of classic ALS. The *kl/kl* is a new animal model of AHC degeneration, and may provide clues to understanding the etiology of classic ALS.

**Keywords** Anterior horn cell · Cytoplasmic RNA · Klotho · Ribosomal RNA gene · Transcription activity

---

# Introduction

Mouse lines exhibiting symptoms of early-onset senescence have been established using insertion mutations; it has been shown that the absence of a single gene produces a variety of aging symptoms. The *klotho* gene has been identified as the causal gene at 5G3 in mice and 13q12 in humans [27]. Homozygotes with the *klotho* gene mutation (*kl/kl*) are reported to demonstrate phenotypes highly similar to human aging, including osteoporosis, calcification of articular cartilage and soft tissue, arteriosclerosis, decreased activity, emphysema, and gonadal, thymic, and dermal atrophy. The life span is reported to be 8–9 weeks on average. The *kl/kl* mice are senescence-accelerated mice satisfying 7 among 21 of the pathophysiological and cellular criteria of aging [27]. An association between the allele of the functional variant of the *klotho* gene and occult coronary artery disease has been reported [3].

In addition to the above-mentioned symptoms, *kl/kl* mice exhibit an abnormal gait. Reduction in the number of cerebellar Purkinje cells [27] may be a factor relating to the gait disturbance, but the spinal cord has not been examined genetically or histologically. To date, there have been no reports on the expression of the *klotho* gene in the spinal cord. An age-related reduction of the number of small neurons in the anterior horn has been reported in humans [25, 26, 40], and it was thus important to examine whether or not similar changes occur in *kl/kl* mice. The purpose of the present study was to clarify the genetic, histological, quantitative and ultrastructural peculiarities in the spinal cord in *kl/kl* mice, and compare those with the findings in the human spinal cord in aging. We have found some degenerative changes, similar to those reported in the human anterior horn cells (AHCs) with neurodegenerative diseases including classic amyotrophic lateral sclerosis (ALS), in this senescence model mouse.

# Materials and methods

## Animals

All animals were bred and kept in a breeder (Clea-Japan Corp., Tokyo, Japan) until just before the sacrifice. At sacrifice, adequate measures were taken to minimize pain and discomfort to the animals, according to the "Guidelines for Experiments of the Tokyo Metropolitan Institute for Neuroscience". All animal experiments conformed to the United States Public Health Service's Policy on Human Care and Use of Laboratory Animals.

The genetic background of the original *klotho* mice was a mixture of C57BL/6J and C3H/J species. We used 21 male *kl/kl* mice and 19 male wild-type (WT) mice at the age of 7 weeks, the period assumed to be that just before death. Genotypes of the sacrificed mice were determined by Southern blot analyses using their tails and probes to detect the inserted plasmid located adjacent to the *klotho* gene locus. The body and brain weights were measured at the time of sacrifice (Table 1). Animals were deeply anesthetized with ether before the processing. For reverse transcription (RT)-PCR, the cervical spinal cords from *kl/kl* and WT mice ($n$=2, respectively) were taken up in lysis buffer for the isolation of total RNA (RNeasy kit; Qiagen, Chatsworth, CA). Fifteen *kl/kl* and 13 WT male mice were transcardially perfused with 4% paraformaldehyde (PFA) in 0.1 M phosphate buffer (PB) (pH 7.3) for paraffin embedding. Four *kl/kl* and 4 WT mice were transcardially perfused with 2.5% glutaraldehyde (GA) and 1% PFA in 0.1 M cacodylate buffer (CB) (pH 7.3) for Epon embedding.

[Table 1 will appear here. See end of document.]

## RT-PCR procedure of the spinal cord

RNA (0.3–1 μg) was dissolved in 30 μl $H_2O$, and the following was added: 2.5 μl 1 M TRIS (pH 7.4), 20 μl 25 mM $MgCl_2$, 2 μl RNase-free DNase (10 U/μl; Roche Molecular Biochemicals, Mannheim, Germany), and 0.5 μl RNasin (40 U/μl; Promega, Madison, WI). The mixture was incubated for 20 min at 37°C and subsequently divided into two parts. In one part, RNA was reverse-transcribed using oligo(dT) primers (Life Technologies, Rockville, MD) and Moloney murine leukemia virus reverse transcriptase (Superscript II; Life Technologies) at 45°C for 1 h. The other part was incubated in the same mixture without the enzyme and was later used as a control for DNA contamination in the PCR. The cDNA was purified (PCR purification kit; Qiagen) and used as a template for PCR in a 60-μl reaction volume containing 1× PCR buffer containing 1.5 mM $MgCl_2$ (Perkin-Elmer, Foster City, CA), 0.2 mM dNTPs, and 0.1 μM of each primer. Specific oligonucleotide primers (Life Technologies) for PCR were designed to amplify rat (GenBank accession no. AB005141) *klotho* mRNA (forward 5'-AGATGTGGCCAGCGATAGTTA-3'; reverse 5'-ACTTGACCTGACCACCGAAGT-3') [29]. A "hot start" was performed manually by adding 1.5 U AmpliTaq (Perkin-Elmer) after an initial incubation of 5 min at 95°C in a thermocycler (Perkin-Elmer, 9700). For each experiment the housekeeping gene glyceraldehyde-3-phosphate dehydrogenase (GAPDH) was amplified with 20 and 22 cycles to normalize the cDNA content of the samples. Equal cDNA amounts were subsequently used for the amplification of *klotho* gene. Amplification was performed for 20–40 cycles (94°C for 30 s, 50°C for 10 s, and 72°C for 90 s). The linear range of amplification was determined for each primer set. The amplicons were analyzed on a 1.5% agarose gel stained with ethidium bromide.

## Histological and immunohistochemical examination

The 5th cervical and 4th lumbar segments were removed from the 4% PFA-fixed spinal cords under a dissecting microscope. Tissue blocks were dehydrated in ethanol series, and embedded in paraffin. Serial transverse sections (6 μm thick) were made, and were subjected to hematoxylin-eosin, Klüver-Barrera (K-B) and pyronin Y preparation.

Sections, 6 μm thick, were also subjected to immunohistochemical staining using the avidin-biotin-peroxidase complex (ABC) method with a Vectastain ABC kit (Vector, Burlingame, CA). The primary antibodies used were rabbit anti-cow ubiquitin polyclonal antibody (dilution

1:150; Dakopatts, Glostrup, Denmark), SMI-31 monoclonal antibody (dilution 1:1,000; Sternberger Monoclonals, Baltimore, MD), and rabbit anti-glial fibrillary acidic protein (GFAP) polyclonal antibody (dilution 1:1,000; Dakopatts). Lectin histochemistry for microglia was performed using IB4 coupled to horseradish peroxidase (HRP) (dilution 1:100, Sigma, St. Louis, MO). Antigenicity was increased for ubiquitin immunostaining by pretreating the sections with 0.025% trypsin for 15 min at room temperature. Endogenous peroxidase activity was quenched by incubating the sections in 3% hydrogen peroxide in methanol and then blocked by incubating for 1 h with 3% normal goat or mouse serum in phosphate-buffered saline (PBS). The sections were incubated with the required primary antibody overnight at 4°C, then incubated with the secondary reagent containing biotinylated anti-rabbit or anti-mouse IgG (diluted 1:200) for 2 h, and finally with the ABC solution for 1 h. The sections were subjected to the peroxidase reaction using freshly prepared 0.02% 3,3'-diaminobenzidine-tetrahydrochloride and 0.005% hydrogen peroxide in 0.05 M TRIS-HCl buffer pH 7.6 for 10 min at room temperature. As antibody controls, the primary antisera were either omitted or replaced with normal rabbit or mouse serum. Several specimens of neural and non-neural tissue from the patients served as positive or negative tissue controls.

## Quantitative examination of the neurons in the ventral spinal gray matter

The number and sectional area of the neurons with nucleus in the ventral part (ventral side of the central canal level; which includes roughly laminae VII, VIII and IX of Rexed's [33] of the 5th cervical gray matter) were examined in three K-B-stained 6-μm-thick sections (12-μm apart to avoid double counting of the neurons) on both sides in 11 *kl/kl* and 10 WT mice. Neurons were identified by the presence of Nissl substance and prominent nucleoli. Sectional neuronal area including cytoplasm and nucleus was measured by a digitizer (Measure 5; System Supply, Nagano, Japan). The number of neurons examined was 2,354 in *kl/kl* and 2,110 in WT mice. The frequency distribution of the cell areas by 40-$\mu m^2$ increments was obtained. Abercrombie's correction factor [1] was applied for split cell error counting. We defined AHCs here as large neurons with a cell area greater than 400 $\mu m^2$, on the basis of their neuronal features and prominent nucleolus in the ventral part of the gray matter.

## Measurement of diameter of nucleoli of neurons in the ventral spinal gray matter

Light microscopic black and white pictures of neurons in the ventral spinal gray matter were taken at 200-fold magnification using K-B-stained 5th cervical segments. The film negatives were magnified 19-fold with a microscopy reader RF-3A (Fuji Film corp. Tokyo, Japan) and diameters of the nucleoli on the screen were measured with the ruler of the microscopy reader. In total, 94 neurons in three *kl/kl* and 87 neurons in three WT mice were examined. The frequency distribution by 0.3-μm increments was obtained.

## Amount of cytoplasmic RNA in the AHCs

The cytoplasmic RNA content was measured in AHCs with nucleolus by the integrated OD of pyronin Y-stained 6-μm-thick sections. The measurement of the pyronin Y-stained area with an image analyzer has been reported as a reliable method for quantitative assessment of RNA [36]. Integrated OD was measured in the cytoplasm in a routine bright field of Zeiss Axiovert 135 with 12 bits camera (Carl Zeiss, Oberkochen, Germany) using the MetaMorph (Universal Imaging. Co., West Chester, PA, USA) software. Measurement was performed in 100 randomly distributed AHCs with nucleolus in *klotho* and WT mice each (10 AHCs/mouse,10 mice each).

## Ultrastructural investigation of the AHCs

Tissue blocks of the 5th cervical cords, fixed with 3% GA-1% PFA in 0.1 M PB, were postfixed with 1% osmium tetroxide, then dehydrated through a graded ethanol series, and embedded in Epon 812. Toluidine blue-stained 1-μm-thick sections were examined using a light microscope, and ultrathin sections of the ventral part of the spinal cords were stained with lead citrate and uranyl acetate and examined using an electron microscope (H9000; Hitachi, Tokyo, Japan) at 100 kV.

## Measurement of transcription activity of rRNA gene in neurons in the ventral spinal gray matter

Silver staining of nucleolar organizer region-associated proteins (AgNORs) [4, 6, 14, 18, 19, 21, 30] was used to evaluate the rRNA gene transcription activity in the neurons in the ventral gray

matter in *kl/kl* and WT mice. PFA-fixed paraffin-embedded 6-μm-thick sections of the 5th cervical segment 12 μm apart were used for the staining.

Microscopic slides were deparaffinized with xylene, dehydrated in an alcohol series, rinsed with tap water, then stained with a 1:2 blended solution of freshly prepared: (i) 2% gelatin in 1% aqueous formic acid and (ii) 50% silver nitrate solution in deionized and distilled water (DDW). The slides were incubated at 37°C in darkness for 20 min, rinsed in DDW, dehydrated with an alcohol series and xylene, and covered with DPX. Areas of AgNOR-positive regions and the nucleus were examined by a digitizer (System Supply, Nagano, Japan), and the ratio was evaluated. Two hundred thirties neurons from four *kl/kl* and 156 neurons from five WT mice were examined.

### Statistical evaluation

Statistical evaluation was performed using the Mann-Whitney U-test to compare the ratio between *kl/kl* and WT mice.

## Results

### Body and brain weights

The body weight of *kl/kl* mice aged 7 weeks was about one-third that of the WT mice, and the brain weight was about four-fifths of the WT mice (Table 1).

### RT-PCR for *klotho* gene expression in the spinal cords

After 40 cycles of RT-PCR, *klotho* gene expression was seen both in WT and in *kl/kl* mice. The expression in *kl/kl* mice was quite weak but significantly positive (Fig. 1). G3PDH was used as control, and the intensities did not differ between *kl/kl* and WT mice. The possibility of DNA contamination as a source of amplified products was believed to be excluded, since the *klotho* gene expression was not seen in the negative control (data not shown).

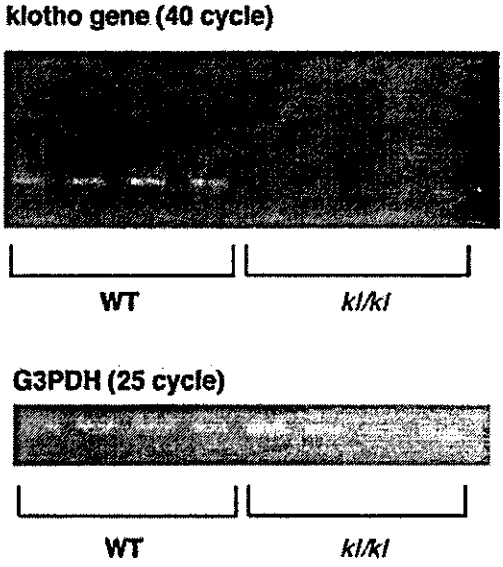


**Fig. 1** *Klotho* gene expression by RT-PCR in the spinal cord. After 40 cycles of RT-PCR, *klotho* gene expression was seen in both WT and in *kl/kl* mice. *klotho* gene expression in *kl/kl* mice is quite weak but significant. G3PDH was used as control, and the intensities were not different between the two genotypes (*RT* reverse transcription, *WT* wild-type, *kl/kl* homozygotes with the *klotho* gene mutation)

## Light microscopic findings of the central nervous system

The neuronal population and size of neurons in the brains of *kl/kl* mice did not show any apparent differences from those of the controls. The cross-sectional area of the gray and white matter of the cervical and lumbar segments of the spinal cord of *klkl* mice was smaller than that in WT mice, in spite of good preservation of the cross-sectional area (Fig. 2A, B) and the neurons of the posterior horn (Fig. 2C, D) of *kl/kl* mice. Large AHCs were seen more frequently in WT than in the *kl/kl* mice, and small neurons were seen more often in the ventral gray matter in *kl/kl* mice (Fig. 2E, F). In the AHCs of *kl/kl* mice, the amount of Nissl substance, i.e., rough endoplasmic reticulum (rER), was smaller (chromatolysis) than that in WT mice (Fig. 2G), and slight but evident accumulation of phosphorylated neurofilaments was observed (Fig. 2I, J). GFAP-immunopositive reactive gliosis was seen in the ventral horn of *kl/kl* mice (Fig. 2K, L), and a moderate increase of number of the IB4-positive cells was seen in the anterior horn in *kl/kl* mice; no significant ubiquitin-immunopositive accumulation, Bunina bodies, or spheroids were observed.

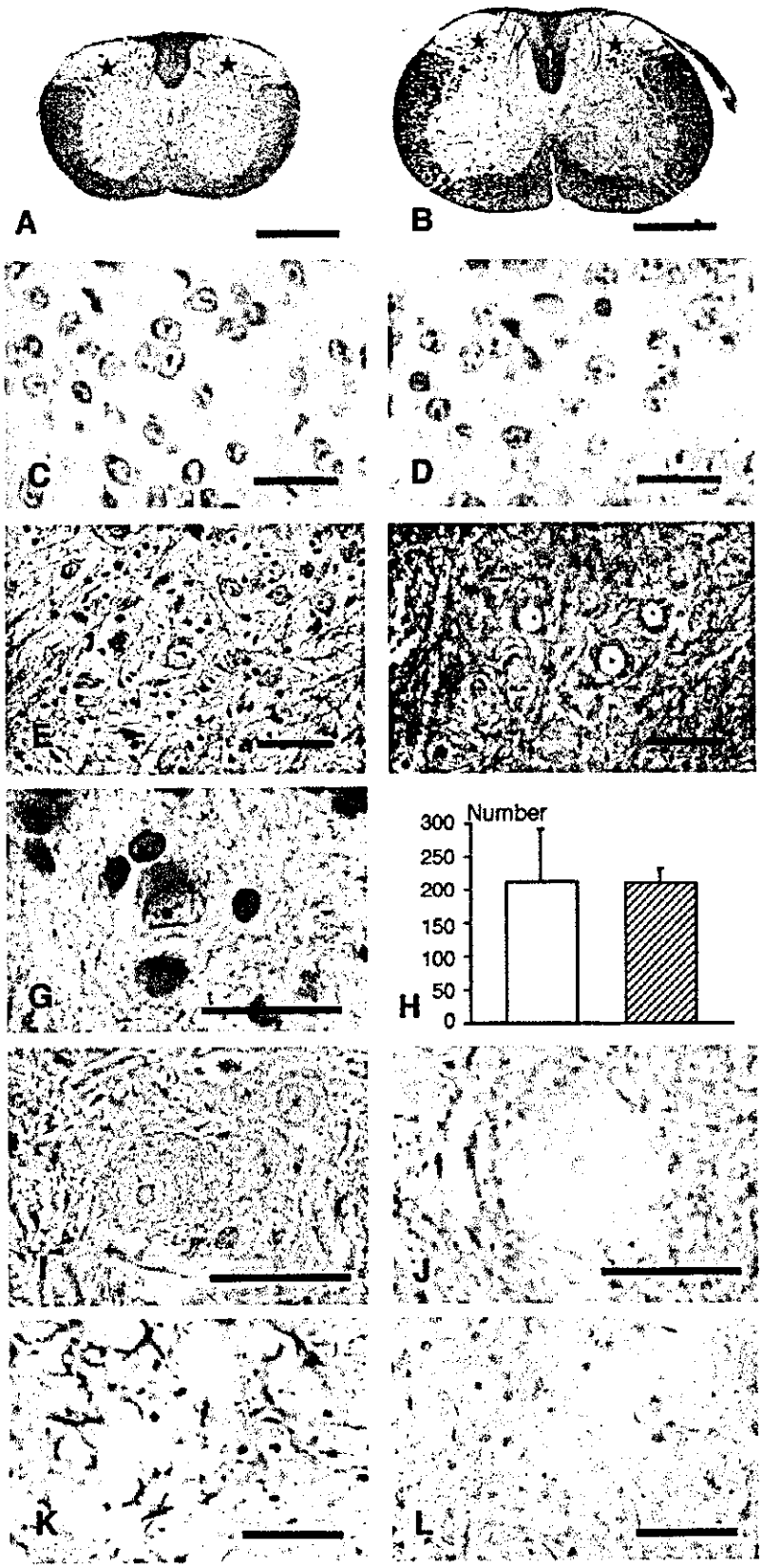


**Fig. 2** Light microscopic findings of the 5th cervical spinal cord. Cross-sectional area of the gray and white matter is smaller in *kl/kl* mice (**A**) than in WT mice (**B**), whereas the posterior horn (*asterisk*) is well preserved

both in area, size and the number of neurons (**C** *kl/kl* mice, **D** WT mice). Large AHCs are seen more frequently in WT mice (**F**) than in *kl/kl* mice (**E**), and small neurons are seen more frequently in the anterior horn in *kl/kl* mice (**E**) than in WT mice (**F**). The amount of Nissl substance in the AHCs in *kl/kl* mice is less than that in WT mice, indicating chromatolysis by the *klotho* insufficiency (**G**). Accumulation of phosphorylated neurofilaments is observed in the AHCs of *kl/kl* mice (**I**) as compared with the WT mice (**J**). GFAP-immunopositive reactive gliosis is seen in the ventral horn of *kl/kl* mice (**K**) as compared with WT mice (**L**). There is no significant difference in the number of neurons in the ventral part of the spinal gray matter between *kl/kl* mice (*open bar*) and WT mice (*hatched bar*) (*error bars* indicate SD) (**H**) (*AHC* anterior horn cell, *GFAP* glial fibrillary acidic protein). **A–G** Klüver-Barrera staining; **I, J** SMI-31-immunohistochemistry; **K, L** GFAP immunohistochemistry. *Bars* **A, B** 0.5 mm; **C, D, G, I, J** 25 μm; **E, F, K, L** 50 μm

## Quantitative examination of neurons in the ventral gray matter

There was no significant difference in the number of the neurons in the ventral part of the spinal gray matter between *kl/kl* and WT mice (Fig. 2H). However, the frequency distribution of the sectional area of the neurons in the ventral gray matter of the 5th cervical cord in the 40-$\mu m^2$ increments showed one peak at 120 $\mu m^2$ in *kl/kl* mice but 160 $\mu m^2$ in WT mice, indicating that the neurons in *kl/kl* mice were smaller (Fig. 3A). The number of large neurons with a cross-sectional area over 400 $\mu m^2$ was significantly lower in *kl/kl* mice than in WT ($P<0.0001$) (Fig. 3B). The highest peaks of distribution frequency by 0.3-μm increments of the diameter of nucleoli of neurons in the ventral spinal gray matter were at 2.1–2.4 μm in *kl/kl* mice, but at 2.7–3.0 μm in WT mice (Fig. 3C). The diameter of neuron nuclei in the ventral spinal gray matter was 2.50±0.91 μm (mean ± SD) in *kl/kl* mice and 2.67±0.77 μm in WT mice; those in *kl/kl* mice were significantly smaller ($P<0.01$).